Arrested shear dispersion and other models of anomalous diffusion

By W. R. YOUNG

Department of Earth, Atmospheric and Planetary Sciences, Massachusetts Institute of Technology, Cambridge, MA 02139, USA

The macroscopic dispersion of tracer in microscopically disordered fluid flow can ultimately, at large times, be described by an advection–diffusion equation. But before this asymptotic regime is reached there is an intermediate regime in which first and second spatial moments of the distribution are proportional to t^ν. Conventional advection–diffusion (which applies at large times) has $\nu = 1$ but in the intermediate regime $\nu < 1$. This phenomenon is referred to as 'anomalous diffusion' and this article discusses the special case $\nu = \frac{1}{2}$ in detail. This particular value of ν results from tracer dispersion in a central pipe with many stagnant side branches leading away from it. The tracer is "held up' or 'arrested' when it wanders into the side branches and so the dispersion in the central duct is more gradual than in conventional advection–diffusion (i.e. $\nu = \frac{1}{2} < 1$).

This particular example serves as an entry point into a more general class of models which describe tracer arrest in closed pockets of recirculation, permeable particles, etc. with an integro-differential equation. In this view tracer is arrested and detained at a particular site for a random period. A quantity of fundamental importance in formulating a continuum model of this interrupted random walk is the distribution of stopping times at a site. Distributions with slowly decaying tails (long sojourns) produce anomalous diffusion while the conventional model results from distributions with short tails.

1. Introduction

The macroscopic spread of a passive scalar in a porous medium, in a shear flow or in a spatially disordered set of streamlines (figure 1) can often be analysed by averaging over microscopic scales or fast variables. This procedure generally yields an effective velocity and an effective diffusivity. Perhaps the first example of this is Taylor's (1953) discussion of unidirectional shear dispersion in a pipe. In this problem the microscopic process is transverse mixing which occurs on a fast timescale, A/κ, where A is the cross-sectional area of the pipe and κ the molecular diffusivity of the scalar. The macroscopic evolution equation is

$$\partial_t f + u\,\partial_x f = D\,\partial_x^2 f, \tag{1.1}$$

where $fA\,\mathrm{d}x$ is the amount of tracer in the pipe between x and $x+\mathrm{d}x$, and u is the sectionally averaged velocity. The effective diffusivity D is given by an expression of the form

$$D = \kappa + \gamma(u^2 A/\kappa), \tag{1.2}$$

where γ is a dimensionless constant ($\gamma = 1/48\pi$ for laminar Poiseuille flow). The original problem was four-dimensional but, after averaging over the cross-section of
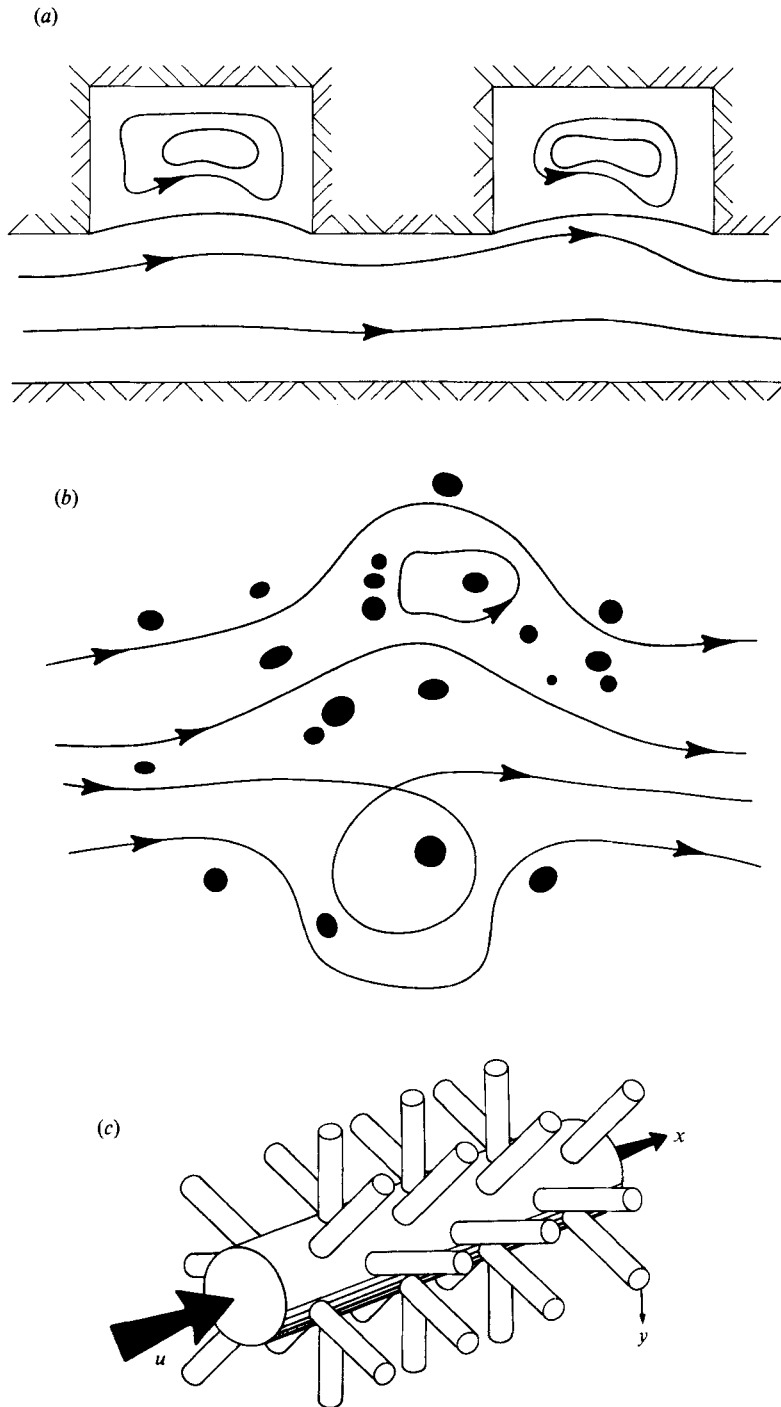
(a)

(b)

(c)

FIGURE 1. Schematic illustrations of different configurations which produce hold-up or arrest. (a) A periodic geometry in which there are regularly spaced, closed streamline regions (e.g. Shen & Floryan 1985). (b) Disordered flow around particles or rods. In addition to the closed streamlines, the particles might be permeable. (c) A central pipe with semi-infinite side branches orthogonal to it. The average spacing between the side branches is l and their sectional area is B.

the pipe, the final evolution equation is two-dimensional. The attractions of this approach are obvious and it is a special example of a considerably more general technique. This is that in many physical problems, after a transient has subsided, the state of a system can be described by a few dominant modes which slowly evolve. This is a centre manifold of finite dimension (Coullet & Spiegel 1983) and in fact Roberts (1988) discusses a simple 'two zone' model of shear dispersion from this perspective.

Taylor's theory has subsequently been generalized beyond its initial focus on shear dispersion in a pipe. Brenner (1980) gives a general procedure for calculating effective velocities and diffusivities in a periodic geometry (e.g. figure 1 a). An interesting application of this formalism to a specific problem is Nadim *et al.* (1986 a). In random geometries, such as creeping flow through packed beds and porous media, macroscopic advection–diffusion models such as (1.1) are still useful and can be obtained using statistical arguments (e.g. Saffman 1959; Koch & Brady 1985).

One limitation of this approach is that it is asymptotic in time: one must wait until the tracer has adequately sampled the underlying, microscopic velocity field. Before this sampling is complete the spread of the tracer is not macroscopically diffusive and cannot be described by a macroscopic diffusion equation such as (1.1). This transient behaviour may be prolonged because the tracer must equilibrate within any persistent closed streamlines of the microscopic velocity fields (Koch & Brady 1985). One says that dispersion of the tracer is 'held-up' or 'arrested' and various examples are illustrated in figure 1. Averaging over the pockets of recirculation is a slow process because it is achieved solely by molecular diffusivity (Rhines & Young 1983).

A signature of the transient regime is that the growth of the second spatial moment of the tracer concentration is not directly proportional to time. Rather it expands as t^ν, and the exact value of ν depends on details of the underlying velocity field. For instance, Guyon *et al.* (1987) argue that in a spatially periodic, two-dimensional series of convection rolls between slippery boundaries, $\nu = \frac{1}{2}$. If the rolls are enclosed by rigid boundaries, $\nu = \frac{2}{3}$ (Pomeau, Pumir & Young 1987). Here, following common usage in statistical physics, this phenomenon is referred to as 'anomalous diffusion'. In this broader context, anomalous behaviour is associated with a random walk on a random lattice (Sahimi *et al.* 1983; Hughes, Montroll & Shlesinger 1982; Derrida & Pomeau 1982).

The calculation of ν in the models above is based on heuristic scaling arguments. The present article analyses a simpler, and much more tractable, model of the non-diffusive transient regime. The configuration is illustrated schematically in figure 1 (c). Fluid flows through a central pipe which has a multitude of smaller tubes branching from it. The side branches are semi-infinite and the fluid within them is stagnant. A tracer is introduced into the central artery and its longitudinal dispersion is observed on times long compared to the transverse molecular diffusion time, A/κ. Of course, without the side branches, this is Taylor's (1932) shear dispersion problem.

The side branches in figure 1 modify (1.1). In §§2 and 3 their effect is analysed in the limit where the longitudinal lengthscale of the tracer distribution, L, vastly exceeds the average spacing, l, of the branches and where A/κ is the fastest timescale in the problem. The longitudinal dispersion of the tracer is then no longer diffusive on macroscopic scales such as L. For instance the centre of mass of the tracer advances downstream, as $(u/\lambda)(\lambda t)^{\frac{1}{2}}$ where λ is an inverse timescale defined in (2.8) below. The width of the distribution about this centre is eventually also proportional to $(u/\lambda)(\lambda t)^{\frac{1}{2}}$, but before this there may be an intermediate regime in which it grows

as $(D/\lambda)^{\frac{1}{2}}(\lambda t)^{\frac{1}{4}}$. The physical explanation is straightforward: when $\lambda t \geqslant 1$ most of the tracer has found its way into the side branches and there it is sheltered from the shear flow which is solely responsible for longitudinal dispersion. Thus the spread of the tracer is arrested by the stagnant, semi-infinite side branches and in this sense their cumulative effect is analogous to pockets of closed recirculation in a spatially disordered flow. The macroscopic effect of this is anomalous diffusion (and anomalous advection).

The above remarks suggest that an important supplement to the analysis of §§2 and 3 is an estimate of how long the side branches must be so that they are 'semi-infinite'. If the invading tracer begins to fill up the branches then the mechanism described above saturates. This is the limit which is captured by the usual averaging procedure in which longitudinal dispersion is diffusive with a macroscopic velocity $\bar{u} \neq u$ and macroscopic diffusivity $\bar{D} \neq D$. This is the subject of §4.

Section 2, 3 and 4 are a complete analysis of a very particular problem. This might serve as a contribution to the understanding of dispersion in branching networks. Of more general significance is whether this specific problem suggests a new class of models which generalize (1.1) and enable one to understand the various types of hold-up illustrated in figure 1. This is the subject of §5 and the conclusion is that there is a class of integro-differential models which are a useful point of departure for future investigations of hold-up.

Finally there are several earlier models of the transient, non-diffusive regime. Most of these (Smith 1981; Gill & Sankarasubramanian 1970, 1972; Roberts 1986) are concerned with unidirectional shear dispersion in which none of the arrest mechanisms in figure 1 operate. There is no anomalous diffusion. Other more general works (e.g. Nadim *et al.* 1986*b*) describe the transient behaviour by a systematic perturbation hierarchy which adds additional terms, such as $\partial_x^4 f$, $\partial_x^6 f$ etc. to the right-hand side of (1.1). It is difficult to say how successful this procedure is at capturing the essentials of hold-up because consistency requires either stopping at (1.1), or including an infinite number of higher-order terms. That is, any finite truncation, except for (1.1), is not consistent as evidenced by the development of negative tracer concentration densities. The connection between this infinite-order perturbation expansion and the integro-differential equation in §§2 and 5 is obscure. But the formulation here is compact and easily analysed. For these reasons it may be preferable to an infinite-order perturbation expansion even though the latter may be more general.

2. The arrested dispersion equation

2.1. *Derivation of the arrested dispersion equation*

Suppose that the tracer is initially injected into the central artery, i.e. there is none in the branches. Further, the initial longitudinal scale, L, is assumed to be much greater than the average distance between the branches, l. Then after a time of order A/κ the tracer evolves according to a modified shear dispersion equation

$$\partial_t(f+g) + u\,\partial_x f = D\,\partial_x^2 f, \qquad (2.1)$$

where $f(x,t)$ is the concentration in the central artery and $g(x,t)$ is the tracer which is hidden in the branches near x at time t. Thus in (2.1) the total amount of tracer between x and $x+dx$ is $(f+g)\,A\,dx$ where A is the cross-sectional area of the central pipe. Only a portion, $fA\,dx$, is actually in the central pipe but it is this which is

advected and shear dispersed by Taylor's mechanism (the second and third terms in (2.1)). The remainder of the tracer, $gA\,dx$, is sequestered in the side branches and once there it does not disperse in the x-direction.

To obtain a closed system, g must be related to f and this is now done by considering the invasion of tracer into an individual branch. If θ is the concentration in a branch then

$$\theta_t = \kappa\theta_{yy}, \quad \theta(0,t) = f(t), \qquad (2.2a, b)$$

is the one-dimensional diffusion problem which governs the spread of tracer in the branch. In (2.2a), y is the local, along-branch coordinate. In the boundary condition (2.2b), $f(t)$ is the changing concentration at the mouth of the branch, in the central artery. The x dependence of f, and through it θ, is understood. An integral representation of the solution of (2.2) is

$$\theta = (4\pi\kappa)^{-\frac{1}{2}}y\int_0^t f(\tau)\exp\{-y^2/4\kappa(t-\tau)\}\,(t-\tau)^{-\frac{3}{2}}d\tau, \qquad (2.3)$$

(e.g. Sneddon 1972). From this, one can readily obtain the total amount of tracer in the branch (the 'inventory')

$$\phi \equiv B\int_0^\infty \theta\,dy, \qquad (2.4a)$$

$$= \kappa^{\frac{1}{2}}B\mathscr{I}^{\frac{1}{2}}f, \qquad (2.4b)$$

where B is the cross-sectional area of the side branches $\mathscr{I}^{\frac{1}{2}}$ denotes an integral operator

$$\mathscr{I}^{\frac{1}{2}}f \equiv \pi^{-\frac{1}{2}}\int_0^t f(\tau)\,(t-\tau)^{-\frac{1}{2}}d\tau. \qquad (2.5)$$

Equations (2.4) and (2.5) state that ϕ is essentially the Abel transform of f. The notation $\mathscr{I}^{\frac{1}{2}}$ is useful because one can show (Whittaker & Watson 1927; Bleistein & Handelsman 1975) that

$$\mathscr{I}^{\frac{1}{2}}\phi = \kappa^{\frac{1}{2}}B\,\mathscr{I}^{\frac{1}{2}}\mathscr{I}^{\frac{1}{2}}f, \qquad (2.6a)$$

$$= \kappa^{\frac{1}{2}}B\mathscr{I}f, \qquad (2.6b)$$

$$= \kappa^{\frac{1}{2}}B\int_0^t f(\tau)\,d\tau. \qquad (2.6c)$$

That is, $\mathscr{I}^{\frac{1}{2}}$ is the square root of the time integration operator, $\mathscr{I}$, defined in (2.6b) and (2.6c). Thus using (2.4) and the time derivative of (2.6c), one can go from f to ϕ and vice versa. This is essentially the solution of the Abel integral equation.

The next step is to relate $g(x,t)$ to $\Sigma\phi$ where the sum denotes all the branches in the vicinity of x. Consider an interval $(x, x+\delta x)$, of volume $A\delta x$, in the central artery. The length δx is at once much greater than l, and much less than L. Thus all the branches in this segment have essentially the same concentration, $f(x,t)$, at their mouths and further there are $\delta x/l$ such branches. From (2.4) the total amount of tracer in the branches is $(\delta x/l)\,\kappa^{\frac{1}{2}}B\mathscr{I}^{\frac{1}{2}}f$. However, by definition, this must be equal to $gA\,\delta x$ so

$$g = \lambda^{\frac{1}{2}}\mathscr{I}^{\frac{1}{2}}f, \qquad (2.7)$$

where
$$\lambda \equiv B^2\kappa/l^2A^2, \qquad (2.8)$$

is an important inverse timescale for the macroscopic evolution of the tracer.

Equations (2.1) and (2.7) are the 'arrested dispersion equations'. It is possible to eliminate the integral operator (see Appendix A) but in many applications it is

probably simplest to work with the system above. This is done in the next section where the initial-value problem is solved quite simply by taking spatial moments of (2.1) and (2.7).

Before doing this, it may be helpful to summarize the approximations made to obtain (2.1) and (2.7). There are three of these. First A/κ must be a fast timescale because (2.1) is a simple modification of Taylor's shear dispersion equation. This is the case if $\lambda^{-1} \gg A/\kappa$ or equivalently $l^2 A \gg B^2$. This is a restriction solely on the geometry of the system. Second is the assumption that it is possible to average over many branches and use $f(x,t)$ as a concentration boundary condition at the mouth of an individual branch. This is valid provided $L \gg l$ and $B^{\frac{1}{2}}$. The final, and perhaps most interesting, assumption is that the side branches are semi-infinite, i.e. (2.3) and its consequence (2.4) are accurate. This assumption is quantitatively assessed in §4.

2.2. *An example of the application of* (2.4)

To conclude this section, (2.4) is used to calculate the amount of tracer injected (the 'inventory') by a simple boundary condition

$$f(t) = 1 \quad \text{if } 0 \leqslant t \leqslant T, \tag{2.9a}$$

or
$$f(t) = 0 \quad \text{if } T \leqslant t. \tag{2.9b}$$

This example is intended to make the notion of a fractional integral more intuitive and familiar. Additionally we note that from (2.2) there is also a very simple expression for the centre of mass of the inventory, namely

$$\bar{y} \equiv \int_0^\infty y\theta \,\mathrm{d}y \bigg/ \int_0^\infty \theta \,\mathrm{d}y,$$
$$= \kappa^{\frac{1}{2}} (\mathscr{I}f / \mathscr{I}^{\frac{1}{2}} f). \tag{2.10}$$

Together (2.4) and (2.10) provide a gross, qualitative description of the evolution of the tracer in the side branch.

With f in (2.9) it is easy to evaluate $\mathscr{I}^{\frac{1}{2}} f$ and one finds

$$\phi = 2B \,(\kappa t/\pi)^{\frac{1}{2}} \qquad \text{if } t < T, \tag{2.11a}$$

or
$$\phi = 2B \,(\kappa/\pi)^{\frac{1}{2}} [t^{\frac{1}{2}} - (t-T)^{\frac{1}{2}}] \quad \text{if } t > T. \tag{2.11b}$$

The inventory initially grows as $t^{\frac{1}{2}}$ but then, after f is switched off, it decreases as tracer escapes from the branch. Ultimately it decays as $t^{-\frac{1}{2}}$. From (2.10)

$$\bar{y} = \tfrac{1}{2}(\pi\kappa t)^{\frac{1}{2}} \qquad \text{if } t < T, \tag{2.12a}$$

or
$$\bar{y} = \tfrac{1}{2}(\pi\kappa)^{\frac{1}{2}} [(t)^{\frac{1}{2}} + (t-T)^{\frac{1}{2}}] \quad \text{if } t > T, \tag{2.12b}$$

and so eventually the centre of mass of the diminishing inventory recedes to infinity.

This behaviour is characteristic of a variety of examples. For instance, if $f = \exp(-\mu t)$, then initially the inventory increases as $t^{\frac{1}{2}}$ but at $t = 0.854 \,\mu^{-1}$ it peaks at a maximum value of $0.541 \, B\kappa^{\frac{1}{2}}$ and thereafter decays.

The asymptotic behaviour of ϕ and $\bar{y}$ at large times can easily be obtained by expanding $(t-\tau)^{\frac{1}{2}}$ in (2.5). One has as $t \to \infty$

$$\mathscr{I}^{\frac{1}{2}} f \sim \left[\int_0^t f(\tau) \,\mathrm{d}\tau + (2t)^{-1} \int_0^t \tau f(\tau) \,\mathrm{d}\tau + \dots \right] \bigg/ (\pi t)^{\frac{1}{2}}, \tag{2.13}$$

provided the various moments,

$$\int_0^\infty f(\tau)\,\tau^n\,\mathrm{d}\tau,$$

exist. Thus generally the inventory will decay as $t^{-\frac{1}{2}}$ and the centre of mass will move to infinity as $t^{\frac{1}{2}}$.

3. Solution of the arrested dispersion equation

3.1. *Spatial moments of the arrested dispersion equation*

In this section the initial-value problem

$$\partial_t(f+g) + u\partial_x f = D\partial_x^2 f, \quad g = \lambda^{\frac{1}{2}}\mathcal{I}^{\frac{1}{2}}f, \tag{3.1 a, b}$$

$$f(x, 0) = f_0(x), \quad g(x, 0) = 0, \tag{3.1 c, d}$$

is solved using the moment method (Aris 1956). Let

$$\langle\bullet\rangle \equiv \int_{-\infty}^\infty \bullet\,\mathrm{d}x, \tag{3.2}$$

and assume that the initial condition has

$$\langle f_0\rangle = 1, \quad \langle xf_0\rangle = 0. \tag{3.3}$$

Note that because of (3.3a), f and g have the dimensions (length)$^{-1}$. This is a convenient assumption which should cause no confusion provided one recalls that $\delta(x)$ also has dimensions (length)$^{-1}$.

The first spatial moment of (3.1) is

$$\langle f+g\rangle = 1, \quad \langle g\rangle = \lambda^{\frac{1}{2}}\mathcal{I}^{\frac{1}{2}}\langle f\rangle. \tag{3.4 a, b}$$

The first of these is simply conservation of the tracer. The second relates the amount in the branches to that in the central artery. Using $\mathcal{I}^{\frac{1}{2}}\mathcal{I}^{\frac{1}{2}} = \mathcal{I}$ one can turn the integral equation (3.4) into a first-order linear differential equation. The solution is

$$\langle f\rangle = \mathrm{e}^{\lambda t}\,\mathrm{erfc}\,[(\lambda t)^{\frac{1}{2}}], \tag{3.5 a}$$

$$\sim (\pi\lambda t)^{-\frac{1}{2}} \quad \text{if } \lambda t \gg 1, \tag{3.5 b}$$

and this is shown in figure 2. Thus as time progresses most of the tracer is found in the branches and very little in the central artery. Note that this result does not exclude the possibility that the amount of tracer in any particular side branch ultimately decreases, say as $t^{-\frac{1}{2}}$. Consistency simply requires that as time increases the tracer is distributed over a larger number of branches.

The first spatial moment (centre of mass) is obtained by multiplying (3.1) by x and then integrating. Thus

$$\partial_t\langle xf + xg\rangle = u\langle f\rangle, \quad \langle xg\rangle = \lambda^{\frac{1}{2}}\mathcal{I}^{\frac{1}{2}}\langle xf\rangle, \tag{3.6 a, b}$$

where $\langle f\rangle$ is given by (3.5a). The solution of (3.6a) is

$$\langle xf\rangle + \langle xg\rangle = (u/\lambda)\,[2\,(\lambda t/\pi)^{\frac{1}{2}} - \langle g\rangle],$$

$$\sim (u/\lambda)\,[2\,(\lambda t/\pi)^{\frac{1}{2}} - 1 + (\pi\lambda t)^{-\frac{1}{2}} + \ldots], \tag{3.7}$$
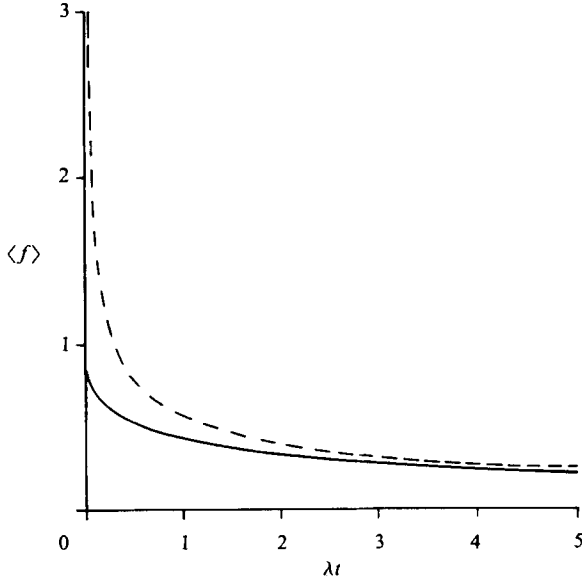
FIGURE 2. The function $\langle f \rangle$ defined in (3.5a) is plotted against time. Also shown (the dashed curve) is the large time approximation in (3.5b).

and this shows that the centre of mass ultimately moves downstream as $t^{\frac{1}{2}}$. The result is not surprising because (3.5) shows that only a small fraction, of order $t^{-\frac{1}{2}}$, is subject to advection when $\lambda t \geqslant 1$. Also of interest is

$$\langle xf \rangle = (u/\lambda)\langle f \rangle(2\lambda t - 1) + (u/\lambda)\{1 - 2(\lambda t/\pi)^{\frac{1}{2}}\}, \tag{3.8a}$$

$$\sim (u/\lambda)[1 - (\pi\lambda t)^{-\frac{1}{2}}], \tag{3.8b}$$

which is obtained by combining (3.6a) and (3.6b) and solving the resulting integral equation. Because the centre of mass is at $\langle xf \rangle + \langle xg \rangle \gg \langle xf \rangle$ this shows that the downstream progress of the centre of mass, given by (3.7), is due entirely to the tracer jumping episodically from one branch to its neighbours. The tracer is continually quitting old branches and invading new ones and it is this process, rather than direct dispersion in the central artery, which spreads the tracer.

The second moment, which is related to the dispersion about the centre of mass, is now obtained by solving

$$\partial_t \langle x^2(f+g) \rangle = 2u\langle xf \rangle + 2D\langle f \rangle, \tag{3.9}$$

and the result is

$$\langle x^2(f+g) \rangle = 4(u/\lambda)^2 \left[\lambda t(\tfrac{3}{2} - \langle g \rangle) + (\lambda t/\pi)^{\frac{1}{2}}(\Delta - 3) + (\tfrac{3}{2} - \tfrac{1}{2}\Delta)\langle g \rangle \right] + \langle x^2 f_0 \rangle, \tag{3.10a}$$

$$\sim 2(u/\lambda)^2 \lambda t + 4(u/\lambda)^2 [\Delta - 2](\lambda t/\pi)^{\frac{1}{2}} + \ldots \tag{3.10b}$$

where
$$\Delta \equiv \lambda D/u^2 \tag{3.11}$$

is a non-dimensional parameter. Validity of (3.10b) requires that $\lambda t \geqslant 1$ but does not suppose any ordering between the two terms on the right-hand side. For instance, it is possible that $u = 0$ in which case the width of the distribution about its centre of mass,

$$\sigma \equiv [\langle x^2(f+g) \rangle - \langle x(f+g) \rangle^2]^{\frac{1}{2}}$$
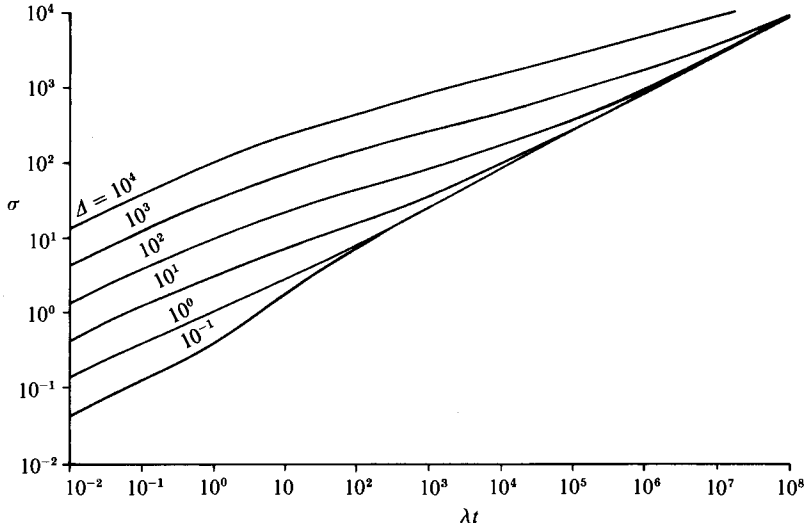
FIGURE 3. The width σ calculated from (3.7a) and (3.10a) with $\langle x^2 f_0 \rangle = 0$. Various values of Δ are shown. At small time $\sigma = (2Dt)^{\frac{1}{2}}$ and all the curves are parallel with slope $\frac{1}{2}$. If $\Delta \gg 1$ there is an intermediate regime with $\sigma \propto t^{\frac{1}{4}}$. This has slope $\frac{1}{4}$ in this ln–ln plot. At large time $\sigma \propto t^{\frac{1}{2}}$ and the curves have slope $\frac{1}{2}$.

grows like $t^{\frac{1}{4}}$ as in Guyon *et al.* (1987). When u is non-zero this anomalous behaviour occurs when the third term in (3.10b) is much greater than the second. The transition, when they are equal, takes place at a time λT given by

$$\lambda T \sim 4\pi^{-1}[\Delta - 2]^2. \tag{3.12}$$

Consistency requires $\lambda T \geqslant 1$ or using (1.1) and noting that $B^2/l^2 A^2$ must be small (see the discussion at the end of §2), this is

$$\lambda T = O\left(\frac{B^2}{l^2 A^2}\frac{\kappa^2}{Au^2}\right). \tag{3.13}$$

Hence the existence of the $t^{\frac{1}{4}}$ regime requires very large values of κ^2/Au^2. These conclusions are summarized in figure 3 which shows σ as a function of time calculated from (3.10a) and (3.7a) using various values of Δ.

The preceeding calculation has provided exact expressions for the spatial moments of the tracer distribution. These suggest that in the two complementary limits $\Delta \gg 1$ and $\Delta \ll 1$, there is a similarity solution for the complete tracer profile. This section is concluded by obtaining these approximate similarity solutions. We begin with the easier case.

3.2. *The limit* $\Delta \ll 1$

If Δ is much less than 1 then lateral diffusion in the central artery is weak and it is plausible that the dominant balance in (3.1a) is

$$\partial_t g + u\,\partial_x f = 0. \tag{3.14}$$

It is clear physically that in this approximation no tracer can move upstream. Applying the operator $\mathscr{I}^{\frac{1}{2}}$ to the above and using (A 4) gives

$$\lambda f + u\,\partial_x g = 0, \tag{3.15}$$

which is the dominant balance in (A 5) when $\varDelta \ll 1$. Now substitution of (3.15) into (3.14) produces a 'one-sided diffusion' equation

$$\partial_t g = H(x)\,(u^2/\lambda)\,\partial_x^2 g, \tag{3.16}$$

where $H(x)$ is the step function which is zero if x is negative and 1 if x is positive. This is the physically appropriate choice of u is positive. The similarity solution of (3.16) which corresponds to a compact initial release is

$$g = (\lambda/u)\,(\pi\lambda t)^{-\frac{1}{2}}\exp\{-x^2\lambda/4u^2t\} \quad \text{if } x > 0, \tag{3.17a}$$

or
$$= 0 \qquad\qquad\qquad\qquad \text{if } x < 0, \tag{3.17b}$$

which satisfies the normalization

$$\int_{-\infty}^{\infty} g\,\mathrm{d}x = 1, \tag{3.18}$$

as in (3.3 a). From (3.17) one can verify that

$$\int_{-\infty}^{\infty} xg\,\mathrm{d}x = 2(u/\lambda)\,(\lambda t/\pi)^{\frac{1}{2}}, \tag{3.19a}$$

$$\int_{-\infty}^{\infty} x^2 g\,\mathrm{d}x = 2(u/\lambda)^2\,\lambda t, \tag{3.19b}$$

which are the results suggested by the moment calculation.

3.3. *The limit* $\varDelta \gg 1$

In this case we set $u = 0$ in (3.1 a) and then tracer moves in the central pipe only because of lateral diffusivity i.e.

$$\partial_t f + \partial_t g = D\,\partial_x^2 f. \tag{3.20}$$

It is also convenient to use (A5) as the second relation between f and g

$$\partial_t g + \lambda f - D\,\partial_x g = \lambda(\pi\lambda t)^{-\frac{1}{2}}\delta(x), \tag{3.21}$$

where, as an initial condition appropriate to a similarity solution, $f(x, 0) = \delta(x)$. An approximate similarity solution to (3.20) and (3.21) is found by substituting

$$g = (\lambda/D)^{\frac{1}{2}}(\lambda t)^{-\frac{1}{4}}G(\eta), \tag{3.22a}$$

$$f = (\lambda/D)^{\frac{1}{2}}(\lambda t)^{-\frac{3}{4}}F(\eta), \tag{3.22b}$$

$$\eta = x/(D^2\lambda^{-1}t)^{\frac{1}{4}}, \tag{3.22c}$$

and retaining only the most slowly decaying powers of t. Thus in (3.20), f_t is negligible and in (3.21) g_t is negligible. Also

$$\delta(x) = (D^2\lambda^{-1}t)^{-\frac{1}{4}}\delta(\eta), \tag{3.23}$$

so that (3.20) and (3.21) reduce to

$$\eta G + 4F_\eta = 0, \quad F - G_{\eta\eta} = \pi^{-\frac{1}{2}}\delta(\eta). \tag{3.24a, b}$$

One can now eliminate F and obtain the equation

$$G_{\eta\eta} + (\tfrac{1}{4}\eta)G = -\pi^{-\frac{1}{2}}\delta'(\eta). \tag{3.25}$$

An integral representation of the solution is constructed and analysed using a Fourier transform in Appendix B. Numerical integration then gives the result in figure 4.

To verify that the similarity solution agrees with the moment calculation one can show from (3.24) that

$$\int_{-\infty}^{\infty} F \, d\eta = \pi^{-\frac{1}{2}}, \quad \int_{-\infty}^{\infty} \eta^2 G \, d\eta = 4\pi^{-\frac{1}{2}}, \qquad (3.26a, b)$$

and these results are all that is needed to demonstrate consistency with (3.5) and (3.10).

Finally, it is interesting to note that because f_t is negligible in (3.20) and g_t is negligible in (3.21) these two combine to give

$$\partial_t g = \lambda^{-1} D^2 \partial_x^4 g + (\pi \lambda t)^{-\frac{1}{2}} D \delta''(x), \qquad (3.27)$$

and the result in figure 4 is the similarity solution of this partial differential equation which is bounded at $x = \pm \infty$. But at first sight (3.27) is not a physical model because it is a 'backwards in time' hyperdiffusion equation, e.g. homogeneous solutions proportional to e^{ikx} grow exponentially. One usually expects hyperdiffusion equations to have a negative coefficient in front of the fourth derivative term (e.g. Gill & Smith 1970). Apparently this is not always so because here is a specific example of a physical problem where the unstable case arises naturally. It is clear that the last term in (3.27), which is related to the persistence of the initial condition, is vitally important in allowing one to construct a solution which is bounded on the real axis. This is because in the homogeneous version of (3.25) only no unbounded solutions on the real axis and the δ' allows one to patch a solution which is bounded at $\eta = \infty$ (and unbounded at $\eta = -\infty$) onto one which has the opposite structure.

4. Finite branches

4.1. *Scaling arguments*

Suppose now that the side branches have finite length, m. Then introducing

$$\mu \equiv \kappa/m^2, \qquad (4.1)$$

we expect that the preceeding calculation is invalid when

$$\mu t = O(1), \qquad (4.2)$$

because by this time the invading tracer will have encountered the end of the branch. When this happens the branch is said to be 'saturated'. Thus if the non-diffusive regimes found in §3 are to be realized then we must have

$$\mu^{-1} \gg t \gtrsim \lambda^{-1} \gg A/\kappa. \qquad (4.3)$$

This requires that $\qquad r \equiv \lambda/\mu = (mB/lA)^2 \qquad (4.4)$

be much greater than one. Thus if μ^{-1} is to exceed λ^{-1} then the volume of a side branch, mB, must be greater than the volume per branch in the central artery, lA.

4.2. *An example: $\Delta \ll 1$*

These estimates will now be illustrated by a specific calculation, based on the profile (3.17). This is the limit $\Delta = \lambda D/u^2 \ll 1$ in which particle transport in the central
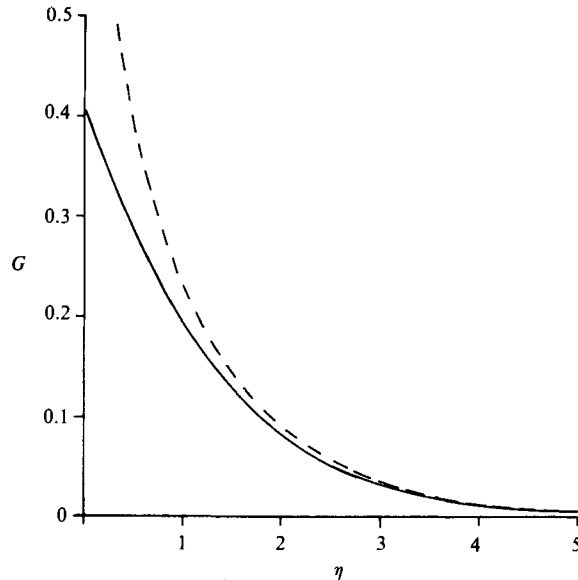
FIGURE 4. The solution of (3.25) with $\eta > 0$. This function is even with a discontinuous derivative at $\eta = 0$. Also shown as a dashed curve is the asymptotic approximation in (B 6).

artery takes place solely by advection. Given g in (3.17), we can calculate f from (3.15) and then use (2.10) to obtain

$$\bar{y}(x) = (\kappa/\lambda)^{\frac{1}{2}}(\pi\lambda t)^{\frac{1}{2}} \exp(\eta^2)\,\mathrm{erfc}(\eta), \qquad (4.5)$$

where

$$\eta^2 \equiv (x\lambda)^2/4u^2\lambda t \qquad (4.6)$$

is the similarity variation. Equation (4.5) is the position of the centre of mass in the branches at x. At fixed x, as $t \to \infty$

$$\bar{y}(x) \sim (\pi\kappa t)^{\frac{1}{2}}, \qquad (4.7)$$

which is the behaviour we anticipate on the basis of the simple calculation in §2.2. Of course when $\bar{y}(x)$ is comparable to m the above calculation is inconsistent. This happens when t is of order $m^2/\pi\kappa$ which is essentially (4.2).

There is perhaps some residual doubt concerning this conclusion. This is because by the time $\bar{y}(x)$ is of order m, there may be very little tracer left in the branch. Perhaps the ends of the branches are never important because those branches which have saturated actually contain a negligible amount of tracer? To support this contention one might note that the branch inventory is proportional to g in (3.17) and at fixed x this ultimately decays as $t^{-\frac{1}{2}}$. Again this behaviour is anticipated on the basis of the simple calculation in §2.2. To dispel this uncertainty it is helpful to calculate

$$\bar{y}^g = \int_0^\infty g\bar{y}\,\mathrm{d}x \Big/ \int_0^\infty g\,\mathrm{d}x, \qquad (4.8)$$

i.e. the centre of mass averaged with respect to the concentration. From (3.17) and (4.5) one finds

$$\bar{y}^g = \tfrac{1}{4}(\kappa t)^{\frac{1}{2}}, \qquad (4.9)$$

so that saturation actually does occur in branches which contain a significant amount of tracer and from (4.9) this happens at $t \sim 16 \, m^2/\kappa$. While the order of magnitude is the same as (4.2), this is larger by a factor of 50 than the estimate based on (4.7). This calculation in (4.9) is probably a more accurate estimate of the time required before a significant amount of tracer is in saturated branches.

4.3. *The arrested dispersion equation with finite side branches*

It is now straightforward to repeat the calculation in §2 and obtain a generalized form of (2.1) and (2.7) which accounts for the finite length of the branches. One finds

$$\partial_t(f+g) + u\,\partial_x f = D\,\partial_x^2 f, \quad g = \int_0^t K(t-\tau)f(\tau)\,\mathrm{d}\tau, \qquad (4.10)$$

where the kernel, K, is

$$K(t) = \lambda^{\frac{1}{2}}(\pi t)^{-\frac{1}{2}} \sum_{n=-\infty}^{n=\infty} \exp[-n^2/\mu t], \qquad (4.11a)$$

$$= 2(\lambda\mu)^{\frac{1}{2}} \sum_{n=0}^{n=\infty} \exp[-\pi^2\mu t(n+\tfrac{1}{2})^2], \qquad (4.11b)$$

and is related to the Jacobi theta function. For future reference, the Laplace transform of K is

$$\tilde{K}(p) = \int_0^\infty \mathrm{e}^{-pt} K(t)\,\mathrm{d}t, \qquad (4.12a)$$

$$= (\lambda/p)^{\frac{1}{2}} \tanh[(p/\mu)^{\frac{1}{2}}]. \qquad (4.12b)$$

In the limit $\mu^{-1} \gg t$ it is easy to use (4.11a) to show that the results of §§2 and 3 are recovered. In the complementary case $\mu^{-1} \ll t$, (4.11b) is the more convenient and noting from (4.12) that

$$\tilde{K}(0) = \int_0^\infty K(t)\,\mathrm{d}t = (\lambda/\mu)^{\frac{1}{2}}, \qquad (4.13a)$$

$$\equiv r^{\frac{1}{2}}, \qquad (4.13b)$$

one can show that (4.10b) reduces to $g = r^{\frac{1}{2}}f$ and then

$$\partial_t c + u_*\,\partial_x c = D_*\,\partial_x^2 c, \qquad (4.14a)$$

$$c \equiv f+g, \qquad (4.14b)$$

$$(u_*, D_*) = (1+r^{\frac{1}{2}})^{-1}\,(u, D). \qquad (4.14c)$$

The last result, (4.14c), is intuitively plausible if one notes from (4.4) that

$$(1+r^{\frac{1}{2}})^{-1} = lA/(lA+mB), \qquad (4.15a)$$

$$= \frac{\text{volume of the central artery}}{\text{total volume}}. \qquad (4.15b)$$

In this limit the tracer distribution is evolving on a timescale which is much longer than μ^{-1}. Consequently the concentration in each branch is uniform and equal to the concentration at the mouth in the central artery. Thus $g = r^{\frac{1}{2}}f$ and the renormalized velocity and diffusivity in (4.14c) follow. This is the macroscopic, diffusive limit which is much more generally captured by a formulation such as that of Brenner (1980).

I emphasize that to obtain (4.14c) it has been assumed that

$$\mu^{-1} \gg A/\kappa, \tag{4.16}$$

i.e. mixing across the central artery is instantaneous. Reversal of this inequality might lead to very different conclusions such as the possibility that D_* exceeds D.

5. A general class of models

The preceding results suggest that as a general model one should study the system

$$\partial_t f + \partial_t g + u\,\partial_x f = D\,\partial_x^2 f, \quad g = \int_0^t K(t-\tau) f(\tau)\,\mathrm{d}\tau, \tag{5.1a, b}$$

where $K(\tau)$ is a kernel such as $\lambda^{\frac{1}{2}}(\pi t)^{-\frac{1}{2}}$. There are immediately two questions raised by this construction. What is the physical interpretation of the kernel and what are the asymptotic $(t \to \infty)$ properties of (5.1)?

5.1. *Physical meaning of the kernel*

Consider a single molecule of tracer wandering in the central artery, and suppose that its progress is episodically interrupted by some mechanism which arrests it at a particular site. It stops there for a random period before it escapes back into the central artery and resumes its progress. This description is reminiscent of several well-known models in statistical physics where a 'pausing time distribution' is used to model 'traps' (a good review is Montroll & West 1979). A complete discussion of the connection between these models and (5.1) is beyond the scope of the present article.

In the preceding sections, arrest or trapping occurs when the molecule wanders into a branch and its progress in the central artery resumes only when its random walk returns it to the mouth of the branch.

One can easily imagine other mechanisms which arrest tracer. The walls of the central artery might be peppered with sites at which tracer molecules 'stick' until dislodged by particularly large thermal fluctuations. Or the central artery might be a streamtube which winds tortuously through an array of closed persistent eddies as in figure 1. Tracer is arrested when it diffuses from the streamtube into one of the gyres. This might serve as a model of tracer dispersion in the abyssal ocean where bottom topography produces at once closed persistent eddies and currents which thread between them (Bretherton & Haidvogel 1976). Similar pockets of recirculation exist in an unconsolidated porous medium and in this same context tracer can also be arrested by permeable particles (Koch & Brady 1985).

A final example is the periodic array of closed convection cells studied by Guyon *et al.* (1987) and Pomeau *et al.* (1987). In these examples there is no preferred direction for transport $(u = 0)$ and the resulting dispersion on scales much larger than an individual convection cell is similar to the limit $\varDelta \gg 1$ studied in §3.3. Each closed convection cell is in a site at which tracer is arrested.

What is common to all these examples, and what we hope to capture with a model such as (5.1), is that when a molecule is arrested a stochastic process, such as a random walk along the branch, begins. The molecule is released when this process passes through an assigned value. For instance in §2 the position of the molecule in the branch, $y(t)$, is a random variable which is initially zero. The molecule is released when this random variable returns to zero. In this example $y(t)$ is the position of the

molecule but generally it might be its thermal energy or some other fluctuating quantity which must pass through a particular value before the molecule escapes.

Having introduced the notion of arrest with a pause of random length, it remains to relate the probability distribution of these sojourns or 'stopping times' to the kernel in (5.1). The probability distribution of stopping times of duration τ will be denoted by $k(\tau)$. Thus if $N \gg 1$ molecules are simultaneously arrested at $t = 0$ then at $t = \tau$ the number still at the site is $Nk(\tau)$. The function $k(\tau)$ is monotonically decreasing and a simple example is the perennially popular exponential distribution

$$k(\tau) = e^{-\alpha\tau}, \tag{5.2}$$

which governs stopping times in a process with no memory. That is, no matter how long a particle has been arrested, there is a constant probability per unit time, α, of escaping. This example should also make it clear that $k(\tau)$ is the distribution of the stopping times, while the density is $(-dk/d\tau)$. For instance the mean pause is

$$\bar{\tau} = -\int_0^\infty \tau \frac{dk}{d\tau} d\tau = \int_0^\infty k \, d\tau, \tag{5.3}$$

provided the integral exists.

The exponential distribution in (5.2) is clearly not appropriate to the example discussed in §2. In this instance

$$k(\tau) = c^{-1}(\kappa/\pi\tau)^{\frac{1}{2}}, \tag{5.4}$$

where c is an arbitrary constant with dimensions of speed which is included for dimensional consistency. The above non-normalized distribution governs the duration of positive excursions (i.e. $y > 0$) in a random walk. Stratonovich (1967, particularly chapter 2), is a useful reference which discusses the lack of normalization in detail. Our inability to normalize (5.4) is related to the singularity at $\tau = 0$. From the definition of $k(\tau)$ one might have expected that $k(0) = 1$. This is the case in simple examples such as (5.2), but it is too restrictive when non-stationary processes such as diffusion are involved. To interpret (5.4) imagine that a large number of particles simultaneously begin a random walk starting in the neighbourhood of $y = 0$. Suppose further, that particles are removed from the ensemble when they pass through $y = 0$. Thus from (5.3) if there are N particles left at $t = \tau$ there are $\frac{1}{2}N$ at $t = 4\tau$ etc.

From (5.4) the reader may have already anticipated that the kernel in (5.1) is just proportional to $k(\tau)$. To see how this convolution arises suppose that $N(\delta t)\delta t$ particles are arrested when $0 < t < \delta t$, $N(2\delta t)\delta t$ in the interval $\delta t < t < 2\delta t$ and so on. Then at a later time, t, the number at the site is $k(t - \delta\tau)\,N(\delta t)\delta t + k(t - 2\delta t)N(2\delta t)\delta t$ and so on. Thus returning to the continuum model, and arguing that the arrival of tracer molecules at the arrest site is proportional to f, the inventory must be given by an expression of the form

$$\phi = A \int_0^t k(t-\tau)f(\tau)\,d\tau, \tag{5.5}$$

where on dimensional grounds A is a constant with the dimensions of (volume/time). For the example in §2, where k is given by (5.4), $A = Bc$. A can be determined by supposing that $f(\tau)$ is constant so that eventually the site saturates (§4) and its inventory is then $\phi = fV$ where V is the 'effective volume' of the site. It then follows from (5.5) that

$$A = V \Big/ \int_0^\infty k(\tau)\,d\tau = V/\bar{\tau}, \tag{5.6}$$

where $\bar{\tau}$ is the average pause at the site. Next if the arrest sites are scattered along the central artery with an average spacing l, then following the argument in §2

$$g = (V/lA\bar{\tau})\int_0^\infty k(t-\tau)f(\tau)\,\mathrm{d}\tau, \tag{5.7}$$

or, comparing this with (5.1),

$$K(\tau) = (V/lA\bar{\tau})\,k(\tau). \tag{5.8}$$

This is the final result which expresses the kernel in (5.1) in terms of the properties of the arrest sites. It is modified in obvious ways if V and $\bar{\tau}$ are infinite as in §2.

In the next subsection we turn to the asymptotic behaviour of solutions of (5.1) as $t \to \infty$. This analysis will show that waiting time distributions which have a slowly decaying tail, such as $\tau^{-\nu}$, produce anomalous diffusion. The model in §2 is a simple example of how such slowly decaying distributions arise naturally. Mandelbrot (1983) argues that they are generally related to sets of fractal dimension and also cites many empirical examples. He emphasizes that often prolonged observation does not indicate the existence of an exponential cut-off at long times. By contrast (5.2), which is also frequently observed to govern waiting-time distribution, produces conventional diffusion as in (4.14). Accordingly the following analysis treats the two cases $k \sim \mathrm{e}^{-\alpha\tau}$ and $k \sim \tau^{-\nu}$ even-handedly. Both are useful models in different circumstances.

5.2. *The asymptotic solution of* (5.1)

The solution of (5.1) at large times can now be found using Laplace transforms

$$\tilde{f}(p) \equiv \int_0^\infty \mathrm{e}^{-pt}f(t)\,\mathrm{d}t. \tag{5.9}$$

Transforming (5.1) we have

$$p(\tilde{f}+\tilde{g}) + u\,\partial_x\tilde{f} - D\,\partial_x^2\tilde{f} = f_0, \quad \tilde{g} = \tilde{K}\tilde{f}, \tag{5.10a, b}$$

where the convolution theorem has been used and $f_0(x)$ is the initial condition. In terms of the total concentration

$$\tilde{c} \equiv \tilde{f}+\tilde{g}, \tag{5.11}$$

we have

$$p(1+\tilde{K})\,\tilde{c} + u\,\partial_x\tilde{c} - D\,\partial_x^2\tilde{c} = (1+\tilde{K})f_0. \tag{5.12}$$

The strategy is now to take spatial moments of (5.12) and extract the large t behaviour of the moment of c from the small p behaviour of the moments of $\tilde{c}$. This is done using Tauberian theorems and an exhaustive reference is Bleistein & Handelsman (1975). But because we are content to stop at the first term, the simpler result given by theorem 4 in chapter 13 of Feller (1971) suffices in the calculations below.

Using the definition (3.2), the moments of (5.12) are

$$\langle\tilde{c}\rangle = 1/p, \tag{5.13a}$$

$$\langle x\tilde{c}\rangle = u/p^2(1+\tilde{K}), \tag{5.13b}$$

$$\langle x^2\tilde{c}\rangle = [2u^2/p^3(1+\tilde{K})^2] + [2D/p^2(1+\tilde{K})] + \langle x^2f_0\rangle/p, \tag{5.13c}$$

and broadly speaking there are two cases depending on whether $\tilde{K}$ is greater than order 1 or order 1 as $p \to 0$. (Because K is positive definite, $\tilde{K}$ cannot be less than order

1, $p \to 0$.) From (5.8) this distinction can be related to the asymptotic behaviour of stopping-time distribution, $k(\tau)$, as $\tau \to \infty$.

Case (i): Brief stops

The easier case is when

$$\tilde{K} \to s = O(1) \tag{5.14}$$

as $p \to 0$. A canonical example of this is the transform pair

$$K = K_0 e^{-\alpha t}, \quad \tilde{K} = K_0/(p+\alpha), \tag{5.15a, b}$$

in which $s = K_0/\alpha$. But generally, from (5.3) and (5.8), we see that

$$s = V/lA, \tag{5.16}$$

provided that the integral defining $\bar{\tau}$ converges, i.e. provided there are not too many long stops. Substitution of (5.14) into (5.13) now shows that $\langle xc \rangle$ and $\langle x^2 c \rangle$ are both directly proportional to time. This is the usual diffusive case and further (5.16) shows that the renormalized velocity and diffusivity is given by (4.14) and (4.15) provided we identify mB with V.

Case (ii): Long stops

This is the more interesting case and in fact it divides into several subcases, one of which is the anomalous diffusion found previously.

But first, in the interests of exhibiting behaviour which contrasts most strongly with case (i), suppose that

$$K(\tau) = K_0, \quad \tilde{K}(p) = K_0/p, \tag{5.17a, b}$$

i.e. the stopping-time distribution does not decay at all. Thus some fraction of the tracer molecules which arrive at a site never leave. One might say the tracer is absorbed. Substitution of (5.17b) into (5.13) is straightforward, but it is even easier to note that (5.1) can be rewritten as

$$\partial_t f + K_0 f + u\, \partial_x f = D\, \partial_x^2 f, \tag{5.18}$$

which shows the exponential attenuation produced by irreversible absorption. It follows that the centre of mass moves only a finite distance, u/K_0, and spread about this centre also eventually ceases. The above result is accurate if $A/\kappa \ll K_0^{-1}$. Stronger absorption is discussed by Smith (1983).

Greater tracer mobility is allowed by the one parameter family

$$K(\tau) = st^{-\nu}, \quad \tilde{K}(p) = s\Gamma(1-\nu)\,p^{\nu-1}, \tag{5.19a, b}$$

where $1 > \nu \geqslant 0$. This kernel corresponds to a fractional integral of order $1-\nu$. It follows from (5.13) that

$$\langle c \rangle = 1, \tag{5.20a}$$

$$\langle xc \rangle \sim [u/s\Gamma(1-\nu)\Gamma(1+\nu)]t^{\nu}, \tag{5.20b}$$

$$\langle x^2 c \rangle \sim [2u^2/s^2\Gamma(1-\nu)^2\,\Gamma(1+2\nu)]t^{2\nu} + [2D/s\Gamma(1-\nu)^2]t^{\nu}, \tag{5.20c}$$

where the first is exact and the remaining two are asymptotic as $t \to \infty$. Strictly speaking it is not consistent to retain the third term in (5.20c) when the second is non-zero (i.e. when $u \neq 0$). This is because it is subdominant and a consistent

calculation would require retention of smaller terms in the expansion of $(1+\tilde{K})^{-1}$. With this proviso, and $s = (\lambda/\pi)^{\frac{1}{2}}$, $\nu = \frac{1}{2}$, (5.20) is in agreement with the results in §3. In particular (3.10b) shows that the coefficient of the third term in (5.20c) is modified by a contribution proportional to u^2 if higher-order terms in the expansion of $(1+\tilde{K})^{-1}$ are retained.

Equation (5.20) shows that the previous results with $\nu = \frac{1}{2}$ are merely a special case of a more general class of anomalous diffusion models. As one intuitively expects, if longer stops become more common $(\nu \to 0)$ then the spread of the tracer is increasingly sluggish. In fact (5.18) is recovered continuously in the limit $\nu = 0$. The other limit, as ν increases, is slightly more subtle. When $\nu > 1$, case (i), with the renormalized velocity and diffusivity, is easily recovered. But on the border between this and (5.20) there is $\nu = 1$ which is the final example studied here.

This case is exceptional as the transform pair

$$K(\tau) = s(1-e^{-\alpha\tau})/\tau, \quad \tilde{K}(p) = s\ln(1+\alpha p^{-1}), \qquad (5.21)$$

indicates. It now follows from (5.13b) that

$$\langle xc \rangle \sim ut/s \ln(\alpha t),$$

and this behaviour is nicely intermediate between conventional advection, in case (i) and fractional advection in (5.20b). From (5.13c) the second moment is

$$\langle x^2c \rangle \sim [u^2t^2/(\ln\alpha t)^2] + [2Dt/\ln\alpha t], \qquad (5.22)$$

so that the width of the distribution about the centre of mass, σ, is proportional to $(t/\ln\alpha t)^{\frac{1}{2}}$. Once again, because the third term in (5.22) is subdominant, the constant of proportionality is probably modified by terms proportional to u^2.

6. Conclusion

Tracer arrest or hold-up can be analysed with the integro-differential model in (5.1). The kernel is directly proportional to the distribution of stopping times at the sites which hold up the tracer. Different mechanisms produce different kernels but the asymptotic $(t \to \infty)$ properties of (5.1) depend only on the behaviour of $k(\tau)$ at large τ. This provides a useful means of classifying different examples and shows that there is a continuous dependence of the model results on changes in $K(\tau)$. Thus at one end of the spectrum there are kernels such as (5.17a) which do not decay at all, and ensure that the tracer remains localized forever in the vicinity of its initial release. The other limit is a rapidly decaying kernel such as (5.15a) and this produces conventional advection–diffusion. In between these two extremes are kernels with relatively slowly decaying algebraic tails such as (5.19a). These produce anomalous advection and diffusion as in (5.20).

Understanding this phenomenon was the initial motivation for this work and the case $\nu = \frac{1}{2}$ has been discussed in some detail in §§2, 3 and 4. The suggestion made there is that this type of behaviour (with perhaps different values of ν) will be characteristic of the various configurations shown in figure 1 – at least until the isolated pockets become saturated with tracer and (1.1) becomes valid. The problem which remains is how to find the kernel appropriate to arrest produced by closed streamlines. The calculation in Pomeau *et al.* (1987) suggests that for convection rolls between rigid boundaries it is of the form (5.19) with $\nu = \frac{2}{3}$. On the other hand, with slippery boundaries, Guyon *et al.* (1987) get $\nu = \frac{1}{2}$ so that there is probably not a unique answer to this question.

Appendix A. Alternative forms of the arrested dispersion equation

We begin by noting some useful results concerning the operator $\mathscr{I}^{\frac{1}{2}}$ defined in (2.5). First

$$\mathscr{I}^{\frac{1}{2}}t^\alpha = [\Gamma(1+\alpha)/\Gamma(\tfrac{3}{2}+\alpha)]\,t^{\alpha+\frac{1}{2}}, \tag{A 1}$$

and in particular

$$\mathscr{I}^{\frac{1}{2}}t^{-\frac{1}{2}} = \pi^{\frac{1}{2}}. \tag{A 2}$$

A useful identity is

$$\partial_t \mathscr{I}^{\frac{1}{2}}f - \mathscr{I}^{\frac{1}{2}}\partial_t f = f(0)\,(\pi t)^{-\frac{1}{2}}, \tag{A 3}$$

so that $\mathscr{I}^{\frac{1}{2}}$ and ∂_t do not commute. Applying $\mathscr{I}^{\frac{1}{2}}$ to (A 3), and using (A 2), gives

$$\mathscr{I}^{\frac{1}{2}}\partial_t \mathscr{I}^{\frac{1}{2}}f = f, \tag{A 4}$$

and it is important to note that this assumes that f does not have any component proportional to $t^{-\frac{1}{2}}$. For example, (A 2) shows that (A 4) is incorrect if $f = t^{-\frac{1}{2}}$. In the applications of (A 4) below f is a non-singular function of time and (A 4) is valid.

Using the above we can obtain an alternative, equivalent formulation of (2.1) and (2.7). Apply $\lambda^{\frac{1}{2}}\mathscr{I}^{\frac{1}{2}}$ to (2.1) and use (A 3) to get

$$\partial_t g + \lambda f + u\,\partial_x g - D\,\partial_x^2 g = \lambda\,(\pi\lambda t)^{-\frac{1}{2}}f(0,x), \tag{A 5}$$

and together with

$$\partial_t g + \partial_t f + u\,\partial_x f - D\,\partial_x^2 f = 0, \tag{A 6}$$

we have a system without any integral operators. For numerical applications this formulation has the advantage of not requiring the retention of f at earlier times.

Appendix B. The solution of the hyperairy equation

To obtain an integral representation of the solution of (3.25) one can use a Fourier transform

$$\tilde{G} \equiv (2\pi)^{-\frac{1}{2}}\int_{-\infty}^{\infty} e^{i\eta\xi}G(\eta)\,d\eta. \tag{B 1}$$

(The notation is the same as Sneddon 1972.) The Fourier transform of (3.25) is

$$\frac{d\tilde{G}}{d\xi} - 4\xi^3\tilde{G} = -(4/\pi\sqrt{2})\,\xi, \tag{B 2}$$

and the solution of this is

$$\tilde{G} = (2\pi)^{-\frac{1}{2}}e^{\xi^4}\,\mathrm{erfc}\,(\xi^2). \tag{B 3}$$

Now using the inversion formula we have an integral representation

$$G = \pi^{-1}\int_0^\infty \cos\eta\xi\, e^{\xi^4}\,\mathrm{erfc}\,(\xi^2)\,d\xi. \tag{B 4}$$

Professor O. G. Ruehr pointed out that this can be put in a more friendly form, viz.

$$G(\eta) = (\sqrt{2}/\pi) \int_0^\infty \exp\left[-\xi^4 - (\eta^2/8\xi^2)\right] d\xi,$$

$$= (\sqrt{2}/\pi) \eta^{\frac{1}{3}} \int_0^\infty \exp\left[-\eta^{\frac{4}{3}}\{\xi^4 + (8\xi^2)^{-1}\}\right] d\xi. \tag{B 5}$$

The first expression is convenient if one needs to extract the small η behaviour while the second is more useful if one needs the large η behaviour. In fact the second case is very straightforward because (B 5b) is the classic form in which Laplace's method produces immediate results

$$G(\eta) \sim (\pi^{-\frac{1}{2}} 3^{-\frac{1}{2}} 2^{\frac{1}{6}}) \eta^{-\frac{1}{3}} \exp\left[-2^{-\frac{8}{3}} 3 \eta^{\frac{4}{3}}\right],$$

$$= 0.366 \eta^{-\frac{1}{3}} \exp\left[-0.472 \eta^{\frac{4}{3}}\right], \tag{B 6}$$

and this is the dashed curve in figure 4.

The small η behaviour follows from (B 5a) and its derivatives. One finds

$$G(\eta) = (\sqrt{2}\,\Gamma(\tfrac{1}{4})/4\pi) - (2\sqrt{\pi})^{-1}|\eta| + (4\Gamma(\tfrac{1}{4}))^{-1}\eta^2 + O(\eta^3), \tag{B 7}$$

and this is what is required to integrate (3.25) numerically starting at $\eta = 0$. This is how the 'exact' result in figure 4 was obtained. The singular term, $|\eta|$, in (B 7) is to be expected because of the δ' in (3.25).

REFERENCES

ARIS, R. 1956 On the dispersion of solute in a fluid flowing through a tube. *Proc. R. Soc. Lond.* A235, 67–77.

BLEISTEIN, N. & HANDELSMAN, R. A. 1975 *Asymptotic Expansions of Integrals.* Dover, 425 pp.

BRENNER, H. 1980 Dispersion resulting from flow through spatially periodic porous media. *Phil. Trans. R. Soc. Lond.* A297, 81–133.

BRETHERTON, F. P. & HAIDVOGEL, D. B. 1976 Two-dimensional turbulence above topography. *J. Fluid Mech.* 78, 129–154.

COULLET, P. H. & SPIEGEL, E. A. 1983 Amplitude equations for systems with competing instabilities. *SIAM J. Appl. Maths* 43, 776–821.

DERRIDA, B. & POMEAU, Y. 1982 Classical diffusion on a random chain. *Phys. Rev. Lett.* 48, 627–630.

FELLER, W. 1971 *An Introduction to Probability Theory and its Applications,* vol. 2. Wiley 669 pp.

GILL, W. M. & SANKARASUBRAMANIAN, R. 1970 Exact analysis of unsteady advection diffusion. *Proc. R. Soc. Lond.* A316, 341–350.

GILL, W. M. & SANKARASUBRAMANIAN, R. 1972 Dispersion of nonuniformly distributed time variable continuous sources in a time-dependent flow. *Proc. R. Soc. Lond.* A327, 191–208.

GILL, A. E. & SMITH, R. K. 1970 On similarity solutions of the differential equation $\psi_{zzzz} + \psi x = 0$. *Proc. Camb. Phil. Soc.* 67, 163–171.

GUYON, E., HULIN, J. P., BAUDET, C. & POMEAU, Y. 1987 Dispersion in the presence of recirculation zones. Proceedings of *Chaos 1987.* To be published in *Nucl. Phys.*

HUGHES, B. D., MONTROLL, E. W. & SHLESINGER, M. F. 1982 Fractal random walks. *J. Stat. Phys.* 28, 111–126.

KOCH, D. L. & BRADY, J. F. 1985 Dispersion in fixed beds. *J. Fluid Mech.* 154, 399–427.

MANDELBROT, B. B. 1983 *The Fractal Geometry of Nature.* Freeman, 468 pp.

MONTROLL, E. W. & WEST, B. J. 1979 On an enriched collection of stochastic processes. In *Fluctuation Phenomena* (ed. E. W. Montroll & J. L. Lebowitz).

NADIM, A., COX, R. G. & BRENNER, H. 1986a Taylor dispersion in concentrated suspensions of rotating cylinders. *J. Fluid Mech.* 164, 185–215.

NADIM, A., PAGITSAS, M. & BRENNER, H. 1986*b* Higher-order moments in macrotransport processes. *J. Chem. Phys.* **85**, 5238–5245.

POMEAU, Y., PUMIR, A. & YOUNG, W. R. 1987 Transients in the advection and diffusion of impurities. *C.R. Acad. Sci. Paris.* to be published.

RHINES, P. B. & YOUNG, W. R. 1983 How rapidly is a passive scalar mixed within closed streamlines? *J. Fluid Mech.* **133**, 133–145.

ROBERTS, A. J. 1988 The application of centre manifold theory to the evolution of systems which vary slowly in space. *Bull. Austral. Math. Soc.* **B** (to appear).

SAFFMAN, P. N. 1959 A theory of dispersion in porous media. *J. Fluid Mech.* **6**, 321–349.

SAHIMI, M., HUGHES, B. D., SCRIVEN, L. E. & DAVIS, H. T. 1983 Stochastic transport in disordered systems. *J. Chem. Phys.* **78**, 6849–6864.

SHEN, C. & FLORYAN, J. M. 1985 Low Reynolds number flow over cavities. *Phys. Fluids* **28**, 3191–3202.

SMITH, R. 1981 A delay-diffusion description for contaminant dispersion. *J. Fluid Mech.* **105**, 469–486.

SMITH, R. 1983 Effect of boundary absorption upon longitudinal dispersion in shear flows. *J. Fluid Mech.* **134**, 161–177.

SNEDDON, I. N. 1972 *The Use of Integral Transforms.* McGraw Hill, 539 pp.

STRATONOVICH, R. L. 1967 *Topics in the Theory of Random Noise*, vol. 2. Gordon and Breach, 329 pp.

TAYLOR, G. I. 1953 Dispersion of soluble matter in solvent flowing slowly through a tube. *Proc. R. Soc. Lond.* A**219**, 186–203.

WHITTAKER, E. T. & WATSON, G. N. 1927 *A Course of Modern Analysis*, 4th edn. Cambridge University Press, 608 pp.